$3D$-TRANSITION OF THE WAKE FLOW BEHIND A HEATED CYLINDER

Camilo C.M. Rindt
Department of Mechanical Engineering, Eindhoven University of Technology
P.O.Box 513, 5600 MB Eindhoven, The Netherlands
c.c.m.rindt@tue.nl

Walfred J.P.M. Maas and Anton A. van Steenhoven
Department of Mechanical Engineering, Eindhoven University of Technology
P.O.Box 513, 5600 MB Eindhoven, The Netherlands

ABSTRACT

The $3D$-transition of the wake flow behind a heated cylinder is studied experimentally using flow visualization. The Reynolds number is fixed at $Re_D = 115$ and the Richardson number is varied between $Ri_D = 0$ (forced convection case) and $Ri_D = 1.5$ (mixed convection case). Visualization experiments are carried out in a towing tank facility with water as the working fluid. From the results it is seen that mushroom-type structures appear on top of the upper vortex row leading to an early breakdown of the vortex street. The appearance of these mushroom-type structures occurs more upstream for higher Richardson values. From detailed visualization experiments it is concluded that the spanwise distribution of these structures is determined in the wake of the heated cylinder close to the cylinder wall.

INTRODUCTION

The stability of the wake behind an 'unheated' cylinder has been the subject of many studies over more than a century. Recently, there is a renewed interest into this classical problem. For $Re_D < 50$ the wake consists of two counter rotating vortices. For $50 < Re_D < 190$ the wake flow is characterized by alternately shed vortices. The wake oscillations are purely periodic within this Reynolds range if parallel vortex shedding takes place. For $190 < Re_D < 250$ $3D$-mode development takes place known as the A-mode and B-mode of instability. Special attention to this transition from a $2D$-state towards a $3D$-state for the forced convection case is given in Williamson (1996).

Despite the fact that mixed convection around bluff bodies is of great importance for various engineering applications (electronics cooling, compact heat exchangers) wake stability for a heated cylinder has until now received very little attention compared to the forced convection case. All previous studies were focussed on the first transition from a $2D$ steady to a $2D$ periodic wake (or *vice versa*). For example Chang and Sa (1990) studied the effect of a heat input on the vortex shedding when buoyancy is acting in the direction of the flow. It was observed that buoyancy tends to decrease the unsteadiness in the wake, finally leading to full suppression of the vortex street. To the best of our knowledge, the influence of heat input on the stability and, moreover, on the $3D$-transition of the wake behind a heated cylinder subjected to a horizontal cross-flow has not yet been investigated.

PROBLEM DESCRIPTION

In figure 1:top the results of a hydrogen bubble visualization of the wake behind a heated cylinder for $Ri_D = 0.5$ (a measure for the importance of buoyancy forces) and $Re_D = 75$ is shown. The remarkable downward deflection of the vortex street is caused by a strength difference between the upper and lower vortices. Besides this negative deflection, the strength difference also leads to a relative motion of two subsequently shed structures. The reason for the strength difference between the upper and lower vortex row lies in the baroclinic vorticity production induced by the heat input. More details about the vortex street behaviour for lower heat inputs ($Ri_D < 1$) can be found in Kieft *et al.* (1998), Kieft *et al.* (1999) and Kieft *et al.* (2000).

The aim of the present study is to investigate the $3D$-transition of the wake behind

a heated cylinder. This $3D$-transition was first visualized for $Ri_D = 1.5$, using a hydrogen bubble technique (see figure 1:bottom). Mushroom-type structures on top of the upper vortex row are observed. Detailed results of this transition process are also obtained using a $3D$ Particle Tracking technique. Besides, more global information was extracted from dye visualizations using a multiple needle probe. Main disadvantage of this method is the discrete positions at which the dye is injected. More information about the preliminary experiments on the $3D$-transition can be found in Kieft (2000). Within the present study more insight into the $3D$-transition process is aimed at using an electro-chemical visualization technique.

RESEARCH METHOD

In Figure 2:left the configuration is shown which is investigated. A cylinder with diameter D is brought to a temperature T_1 and is cooled by a horizontal cross flow with a velocity U_0 and a temperature T_0. The relevant dimensionless parameters are the Reynolds number $Re_D = (U_0\ D)/\nu$, the Richardson number $Ri_D = Gr_D/Re_D^2 = (g\ \beta\ \Delta T\ D)/U_0^2$ and the Prandtl number $Pr = \nu/\alpha$. Here β denotes the expansion coefficient, ν the kinematic viscosity, g the gravity constant, ΔT the temperature difference $T_1 - T_0$ and α the thermal diffusivity.

The experiments are carried out in a towing tank facility with water as the working fluid. A cylinder with a diameter of $D = 8.5\ mm$ is clamped between two endplates which are towed through the tank using a translation system (see figure 2:right). Special emphasis is given to the endplate construction to avoid oblique vortex shedding. To obtain the desired cylinder wall temperature an electric rod heater is used. The temperature of the cylinder is kept constant in time by controlling the heat input. The specific dimensions of the tank are $length \times width \times height = 500\ cm \times 50\ cm \times 75\ cm$. Because in the present study the Reynolds number is fixed at $Re_D = 115$, this results in a maximal measuring time of about 3 min.

Flow visualization experiments are carried out using an electro-chemical method. A thin tin-plate is positioned about $15D$ upstream of the cylinder. The specific dimensions of the plate are $length \times width \times thickness = 200\ mm \times 13\ mm \times 1\ mm$. Due to an applied potential difference tin-ions are dissolved in the water and react towards a metallic salt. Using ordinary light sources like slide projectors the solid tin can be visualized. With more advanced laser techniques also cross sections of the fluid flow can be enlighted. Dependent on the vertical position of the tin-plate the upper or lower vortex rolls are visualized.

Insertion of the tin-plate leads to a disturbance of the inflow conditions for the heated cylinder. The Reynolds number based on the thickness of the tin-plate is around $Re_H = 10$. From an analytical estimation and from numerical calculations it appeared that the main stream velocity at the position of the heated cylinder decreased with about 10 % due to the insertion of the tin-plate. This decrease in main stream velocity can be interpreted as a decrease in the Reynolds number experienced by the heated cylinder. The Reynolds numbers mentioned in the present study are not corrected for this effect and are still based on the undisturbed main stream velocity U_0.

VISUALIZATION RESULTS

Figure 3 shows visualization results of the wake flow for $Re_D = 116$ and $Ri_D = 1$ using a laser-sheet positioned halfway the width of the tank. Clearly visible in the top-figure are the mushroom-type structures on top of the upper vortex row. These structures start to develop at the 3^{rd} upper vortex and stretch in vertical direction when convected downstream. That these structures are really $3D$ can be concluded from the bottom-figure where a snapshot of the wake flow is presented at a different moment in time. In the time-span between both figures the position for the occurrence of the mushroom-type structures has shifted in spanwise direction. In the bottom-figure they are still vaguely visible. In this 'between-plume' visualization the wake flow manifests itself more or less as the regular Von Karman vortex street. Main difference with the Von Karman vortex street is the rotation of the lower vortex underneath the upper one. This rotation is also found in the 'in-plume' visualization.

The above effects like the occurrence of mushroom-type structures on top of the upper vortex row and the rotation of the lower vortex underneath the upper one, were also found by Kieft (2000). To investigate these effects in more detail he performed $2D$ Spectral Element calculations. From the calculations it appeared that these effects could be fully attributed to baroclinic vorticity production in

the region downstream of the cylinder between $1 < x/D < 6$. The baroclinic vorticity production in this region results in stronger upper vortices compared to the lower ones. For low heat inputs this leads to a negative deflection of the complete vortex street. For higher heat inputs baroclinic vorticity production leads to the formation of a dipolar structure in the upper row. This dipolar structure accelerates in positive vertical direction and eventually escapes from its parental structure as a mushroom-type structure. This escape could not be simulated due to its $3D$ character.

In Figure 4 an oblique view from the top is shown of a tin visualization experiment for $Re_D = 117$ and $Ri_D = 0.4$ (left) and $Ri_D = 1$ (right). At the bottom of both figures the cylinder is visible (note the slight difference in magnification factors). The flow is now directed from the bottom to the top. It is seen that for $Ri_D = 0$ parallel shedding takes place. The curvature in the vortex rolls moving downstream can be fully attributed to optical distortions. Besides, small end effects are visible, probably due to the finite length of the tin-plate. From this experiment it can be concluded that for this value of the Reynolds number the vortex street behaves fully $2D$ and that oblique shedding was successfully avoided by the end-plate construction.

For $Ri_D = 1$ again the escape of mushroom-type structures can be observed at downstream positions around $x/D \approx 10$. The spanwise distance between these structures is typically $2D$. More important, however, is the fact that the spanwise locations of these 'thermals' seem to be linked to processes taking place close to the cylinder wall. One can see from the right-figure that the vortex roll closest to the cylinder already shows some slight disturbances in spanwise direction. The reason that these disturbances were not noticed in earlier performed Particle Tracking experiments is probably due to the fact that in the visualization results small differences are integrated in time.

To look into more detail to the processes taking place, a horizontal cross-section is made of the wake flow using a laser-sheet. A camera is focussed on a small area close to the cylinder wall. The tin-plate was positioned in such a way that the visualization dye ended up in the upper boundary layer of the cylinder. In Figure 5 the results are presented for $Re_D = 116$ and $Ri_D = 0$ (top) and $Ri_D = 1$ (bottom). For $Ri_D = 0$ no disturbances in spanwise direction can be observed. For $Ri_D = 1$, however, $3D$-structures are present near the heated cylinder wall. Close examination of the camera images revealed that these $3D$-structures consist out of two counter rotating vortices (in the plane of visualization). These counter rotating vortices seem to be highly linked to the observed deformations of the vortex rolls and vortex braids. The spanwise position of the midplanes of these twin-vortices exactly coincides with the spanwise position of the thermal plumes more downstream. From experiments in which the Richardson number was varied, it is concluded that the above discussed $3D$-transition sets in at $Ri_D \approx 0.3$. The spanwise distance of the vortical structures is hardly influenced by the Richardson number and remains rather constant around a value of $2D$.

CONCLUSIONS AND PROGRESS

In the present investigation results are shown of visualizations of the vortex street behind a heated cylinder and subjected to a horizontal cross-flow. The Reynolds number was set to $Re_D = 115$ and the Richardson number was varied between $0 < Ri_D < 1.5$. The results presented indicate that the flow behind a heated cylinder shows a transition towards a $3D$-state at a lower Reynolds number than the flow behind an 'unheated' cylinder. Note that for the pure forced convection case (no heat input) $3D$-transition occurs at a Reynolds number around $Re_D \approx 180$. Besides, the onset towards a $3D$-state takes place near the heated cylinder wall where counter rotating vortices seem to end up in deformations of the vortex rolls and vortex braids. These deformations finally lead to the escape of thermal like structures from the upper vortex row. Future experiments using $3D$ Particle Tracking and calculations using a Spectral Element code must shed more light onto these $3D$-transition processes.

References

Williamson, C.H.K., 1996, "Three-dimensional wake transition", *J. Fluid Mech.*, Vol. 328, pp. 345-407.

Chang, K.S., and Sa, J.Y., 1990, "The effect of buoyancy on vortex shedding in the near wake of a circular cylinder", *J. Fluid Mech.*, Vol. 220, pp. 253-266.

Kieft, R.N., Rindt, C.C.M., and Steenhoven, A.A.v., 1998, "The influence of buoyancy on the behavior of the vortex structures in a cylinder wake", *Proceedings 11th Interna-*

tional Heat Transfer Conference, J.S. Lee, ed., Vol. 3, pp. 219-224.

Kieft, R.N., Rindt, C.C.M., and Steenhoven, A.A.v., 1999, "The wake behaviour behind a heated horizontal cylinder", *Exp. Thermal and Fluid Science*, Vol. 19, pp. 183-193.

Kieft, R.N., Rindt, C.C.M., and Steenhoven, A.A.v., 2000, "3D-transition of low Reynolds number flow around a heated cylinder", *Proceedings 3rd European Thermal Sciences Conference*, E.W.P. Hahne et al., ed., Edizioni ETS, Pisa, pp 659-664.

Kieft, R.N., 2000, "Mixed convection behind a heated cylinder", *PhD-thesis*, Eindhoven University of Technology, The Netherlands.

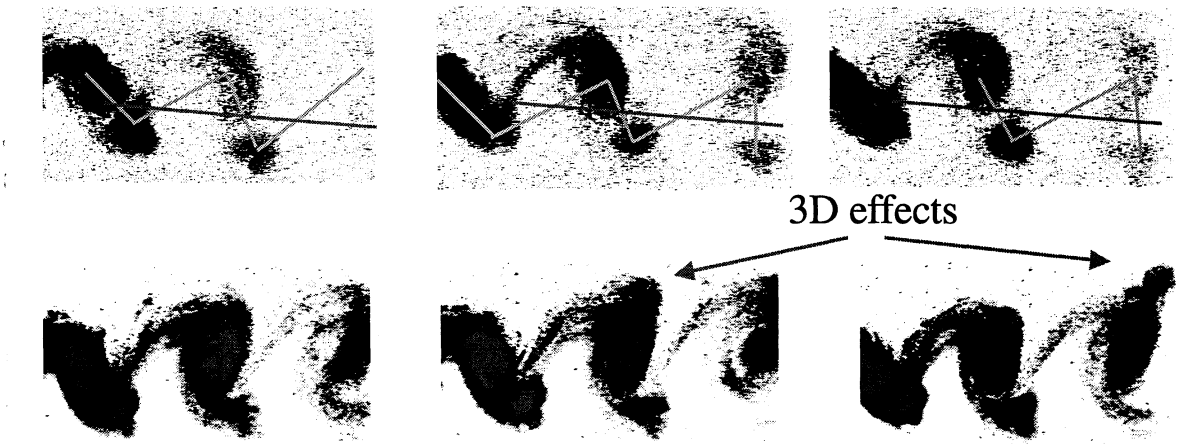

Figure 1: Hydrogen bubble visualizations: side-view. $Re_D = 75$ and $Ri_D = 0.5$ (top) and $Ri_D = 1.5$ (bottom).

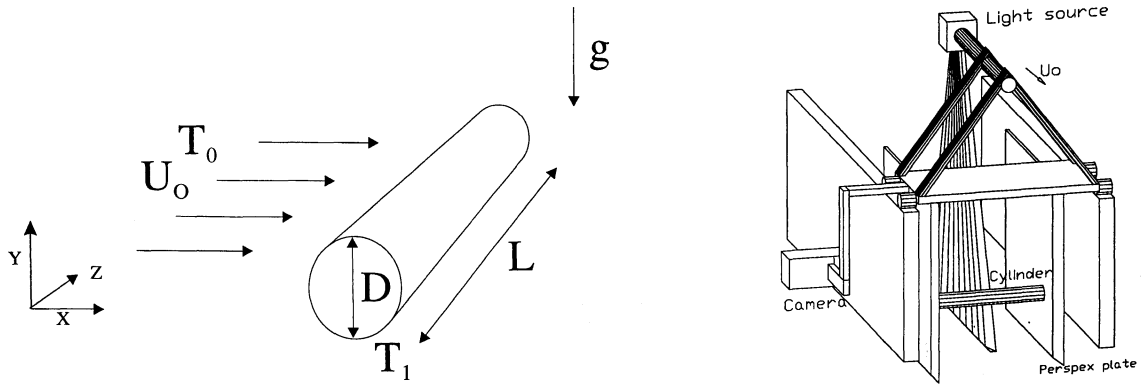

Figure 2: Problem definition (left: the velocity direction is perpendicular to the gravitational direction) and detail of the experimental set-up (right).

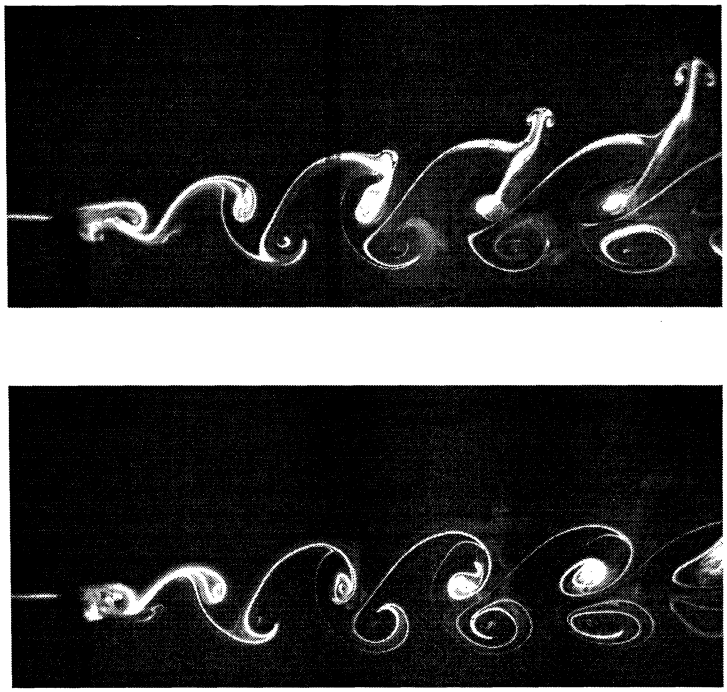

Figure 3: Visualization of the flow behind a heated cylinder: side-view. $Re_D = 116$, $Ri_D = 1$, 'in-plume' visualization (top) and 'between-plume' visualization (bottom).

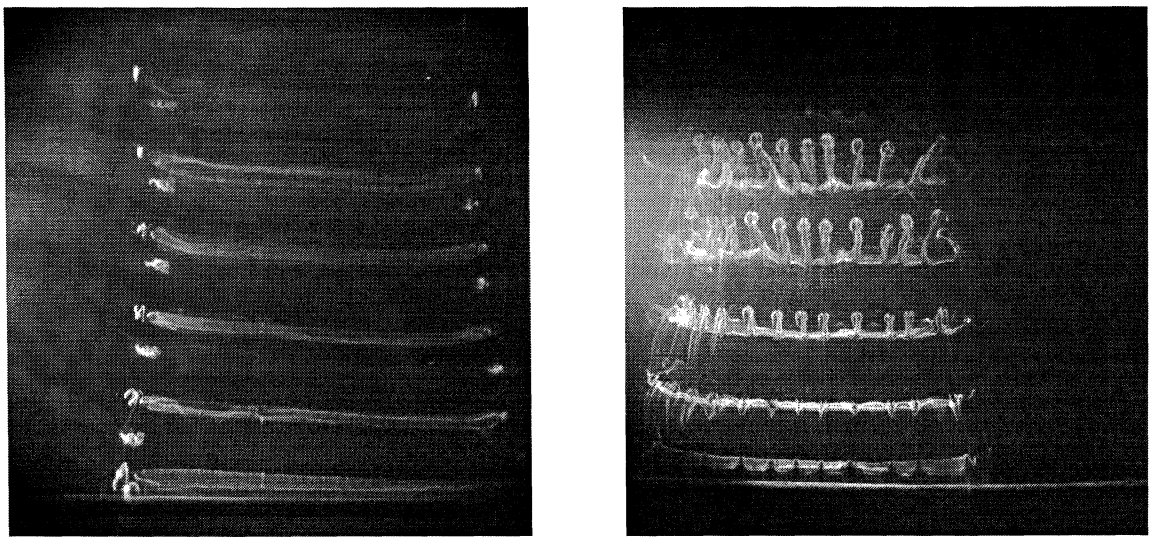

Figure 4: Visualization of the flow behind a heated cylinder: oblique top-view. $Re_D = 117$, $Ri_D = 0$ (left) and $Ri_D = 1$ (right).

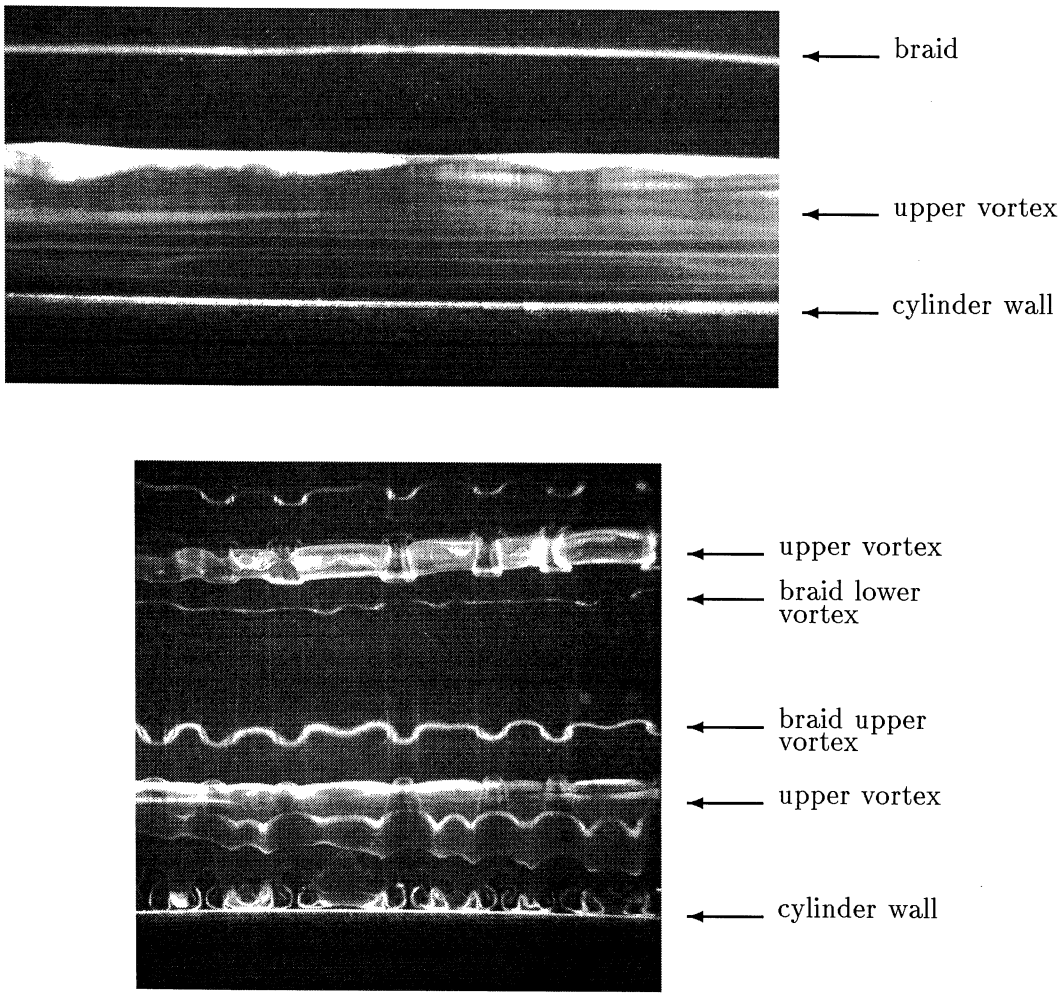

Figure 5: Visualization of the flow behind a heated cylinder: top-view. $Re_D = 116$, $Ri_D = 0$ (top) and $Ri_D = 1$ (bottom).